Estimation of the elastic modulus of child cortical bone specimens

via microindentation

Marie Semaan^{a,b,c}, Elie Karam^b, Cécile Baron^{a,c}, Martine Pithioux^{a,c,*} ^aAix Marseille Univ, CNRS, ISM, Marseille, France; ^bUniversity of Balamand, Faculty of Engineering, Al Kurah, Lebanon; 'Aix Marseille Univ, APHM, CNRS, ISM, Sainte-Marguerite Hospital, Institute for Locomotion, Department of Orthopaedics and Traumatology, Marseille, France *Corresponding author: martine.pithioux@univ-amu.fr, Tel: +33(0) 491745244 Aix-Marseille Université, CNRS, ISM UMR 7287, 13288 Marseille cedex 09, France

ABSTRACT Purpose: Non-pathological child cortical bone (NPCCB) studies can provide clinicians with vital information and insights. However, assessing the anisotropic elastic properties of NPCCB remains a challenge for the biomechanical engineering community. For the first time, this paper provides elastic moduli values for NPCCB specimens in two perpendicular directions (longitudinal and transverse) and for two different structural components of bone tissue (osteon and interstitial lamellae). Materials and Methods: Microindentation is one of the reference methods used to measure bone stiffness. Here, 8 adult femurs (mean age 82±8.9 years), 3 child femurs (mean age 13.3±2.1 years) and 16 child fibulae (mean age 10.2±3.9 years) were used to assess the elastic moduli of adult and children bones by microindentation. **Results:** For adult specimens, the mean moduli measured in this study are 18.1 (2.6) GPa for osteons, 21.3 (2.3) GPa for interstitial lamellae and 13.8 (1.7) GPa in the **transverse** direction. For child femur specimens, the mean modulus is 14.1 (0.8) GPa for osteons, lower than that for interstitial lamellae: 15.5 (1.5) GPa. The mean modulus is 11.8 (0.7) GPa in the **transverse** direction. Child fibula specimens show a higher elastic modulus for interstitial lamellae 15.8 (1.5) than for osteons 13.5 (1.6), with 10.2 (1) GPa in the transverse direction. Conclusion: For the first time, NPCCB elastic modulus values are provided in **longitudinal** and **transverse** directions at the microscale level. **KEYWORDS:** Pediatrics; Cortical bone; Elastic modulus; Microindentation

Introduction

62 63 64

65

66

67

68

69

70

71

72

73

74

75

76

77

78

79

80

81

82

83

84

85

86

87

and formation phases. This enables it to respond to mechanical stimuli, to fix the microdamaged matrix and to adjust the homeostasis of calcium (1). At microscale level, this remodeling forms osteons or Haversian systems, the main structural units in cortical bone. An osteon, a cylinder roughly 200 or 250 µm in diameter, is formed of mineralized collagen fibrils; hydroxyapatite crystals and collagen molecules (2). The crystalline apatite mineral component plays a role in bone strength (3), and the collagen component in plastic deformation (4). The non-osteonal bone is interstitial bone from previous generation of osteons, subperiosteal and subendosteal circumferential lamellae. With age, the portion of osteonal bone increases with respect to the proportion of interstitial bone, as more and more osteons become remodeled (5). Sobol et al. (2015) state that the proportion of osteons with a large diameter of Haversian canals increases with age, due to the activity of osteoclasts and the resorption of the osteon's lamellae during the resorption phase (6). Furthermore, the proportion of osteonal bone to interstitial bone also changes with anatomic site (7). Different osteon characteristics play a role in the microscale elastic properties of bone: collagen fibril orientations (8, 9), levels of mineralization (10, 11) and variations in collagen crosslinking (12). Furthermore, the elasticity of cortical bone is known to be anisotropic at tissue scale, also called mesoscale (13). To gain insight into how microscale elastic properties contribute to mesoscale anisotropy, one of the reference techniques used is microindentation. This allows the elastic modulus to be determined in several directions at microscale level (14, 15, 16, 17). Microindentation involves applying a force on a polished specimen surface by a Berkovich diamond-tip indenter, enabling indentation modulus assessment. The literature reports wide use of microindentation on adult bone (9, 18, 19, 20, 21, 22) to investigate microscale anisotropy by assessing the elastic moduli in different directions. However, the few existing studies on child bone limited their explorations to the **longitudinal** direction (23, 24, 25, 26). The reasons for this limitation are the lack of bone pieces available and their irregular

Bone is a multi-scale living tissue engaged in a continuous remodeling process of successive resorption

shape and small size, an additional challenge in terms of preparing experimentally usable samples. Moreover, all the studies on child bone using microindentation were conducted on pathological specimens embedded in epoxy resin, to facilitate the achievement of a flat and smooth surface (23, 25). However, resin has been demonstrated to affect microindentation measurements by increasing the indentation modulus (27).

This article is the first to provide elastic moduli values for NPCCB specimens in two perpendicular directions (**longitudinal** and **transverse**) and for two different structural components of bone tissue (osteon and interstitial lamellae).

8 adult femurs (mean age 82±8.9 years) were collected from corpses at the Timone Hospital (Marseille,

Materials and methods

Specimen preparation

France). 19 child bone pieces from 16 fibulae (mean age 10.2±3.9 years) and 3 femurs (mean age 13.3±2.1 years) were recovered during bone-lengthening surgery in the Timone hospital. Both adult and child specimens were collected from the distal 1/3 of the femur, and child specimens from the distal 1/3 of the fibula. The children were free of pathologies affecting bone quality and were not bedridden. The National Commission for Data Protection and Liberties (CNIL-France) accepted the experimental protocol and ethical approval was granted by the anatomy laboratory. Informed consent was obtained from the children's legal representatives.

The specimens of child bone, the longest being under 2 cm, were cut into rectangular parallelepipeds by a water-cooled low-speed diamond saw (Buehler Isomet 4000, Buehler, Lake Bluff, IL, USA). Throughout cutting, the bone was hydrated with buffered saline (28). The mean dimensions of these specimens along the radial, circumferential and longitudinal directions, respectively, are the following: adult femurs: 2.2±0.5×5.8±0.6×10.7±1.9 mm³, child fibulae: 1.4±0.6×2.9±0.8×4.5±1.5 mm³ and child femurs: 0.9±0.4×3±0.3×6.4±3 mm³. To ensure the parallelism of bone specimens, a specimen holder

was especially developed for the cutting phase and adapted to the diamond saw. The direction of the medullary canal, assumed to be parallel to the Haversian canals in long bones, was considered as **longitudinal** and the **perpendicular direction to this canal as the transverse direction**. The osteons and interstitial lamellae were only distinguishable from each other in planes perpendicular to the **longitudinal** direction (Figure 1). Consequently, the elastic modulus of the osteon and interstitial lamellae were measured separately only in the **longitudinal** direction (Tables 1 and 2).

Specimens were stored at -20°C (29) after cutting. The specimens' surfaces were smoothed using silicon carbide abrasive paper (grit # 1200) under deionized water and then polished using a 1µm diamond suspension. After each side (**longitudinal** and **transverse**) was polished, the specimen was cleaned with water in an ultrasonic cleaner system (Elma/DE-78224 Singen, Germany) to remove the polishing dust. During microindentation measurement, they were fully hydrated and maintained at room temperature (~23°C).

Microindentation

- The microindentation equipment used (Tester NHT^2 , Anton Paar, Switzerland and Austria) provides an elastic indentation modulus at microscale level with a Berkovich diamond tip displaced in the vertical direction.
- A fused silica reference sample was used to calibrate the tip contact surface. Each indentation was performed with a maximum load of 40 mN and at identical loaded and unloaded rates of 80 mN/min, separated by a 10 s pause. The hold period of 10 s was intended to stabilize any creep in the specimens and to avoid the formation of the common 'nose'-shaped load displacement curve responsible for inaccurate calculations of the unloading curve section (30). The distance between two indentations was 20 μ m, with a maximum (contact) depth of 2 μ m.

Theory

The Oliver-Pharr method is a well-documented way of determining the elastic modulus from the unloading curve, using the assumptions for a linear elastic isotropic material (31). Stiffness (S) reflects

the measurement of bone resistance to an elastic deformation (16). It characterizes the force-displacementrelation:

$$S = \frac{dF}{dh} = \frac{2}{\sqrt{\pi}} \beta E r \sqrt{Ac} , \qquad (1)$$

where F is the force applied, h is the total displacement at any time during loading, β is a correction factor for the unaxisymmetric indenter and is equal to 1.034, Er is the reduced modulus, Ac is the projected area of contact (Ac=24,5 hc² for Berkovich indenter, h is the contact depth of the indenter with the sample at Fmax). The measurement of Er from Equation (1) leads to the elastic modulus of the bone, E*:

146
$$E^* = \frac{1 - v_s^2}{\frac{1}{E_T} - \frac{1 - v_i^2}{E_i}},$$
 (2)

where v_s is the Poisson ratio of the bone (v_s =0.3), E_i is the elastic modulus of the indenter tip (E_i = 1141 GPa) and v_i is the Poisson ratio of the indenter (v_i = 0.07).

Maps of indentations

In this study, 80 indentations per specimen were distributed in the **longitudinal** direction as follows: 20 in an osteon, 40 in two different interstitial lamellae and 20 in a neighboring osteon. Thus, 50 indentations per specimen were performed in the **transverse** direction without distinguishing between osteon and interstitial lamellae, which cannot be differentiated from each other in the **transverse** direction (32). Typical indentations in the **longitudinal** direction and in the **transverse** direction for a 15-year-old child

Of these 3510 indentations, 20% were excluded from the analysis, mainly because they could not be

are shown in Figure 1. In summary, 130 indentations were performed on each of the 27 bone specimens.

clearly identified as belonging to either the osteon or the interstitial regions in the longitudinal direction.

Some were excluded because their load-depth curve showed irregularities (9).

Statistical analysis

Data are reported as mean and standard deviations unless otherwise stated. The analyses were based on three different categories: adult (femur), child (femur) and child (fibula). Statistical analyses were performed using Xlstat (v 2014.1.08, Addinsoft. 2016. XLSTAT, 2016: Data Analysis and Statistical

Solution for Microsoft Excel, Paris, France (2016)). Normality was tested via the Shapiro-Wilk procedure and equality of variances via the Fisher test. Differences between adult (femur) and child (femur) groups were tested using the Mann-Whitney test. Bivariates correlations between the elastic moduli of child fibulae and age were tested by the Spearman's rank correlation test (r). Differences between locations and directions (longitudinal osteon, longitudinal interstitial lamellae and transverse) were tested using the Wilcoxon test. A two-tailed significance level of 0.05 was used. **Results** For child femur specimens, the mean modulus is 14.1 (0.8) GPa for osteons, which is lower than interstitial lamellae, 15.5 (1.5) GPa. The mean modulus is 11.8 (0.7) GPa in the transverse direction (Table 1). The fibula also has a lower modulus in osteonal bone 13.5 (1.6) GPa compared to interstitial 15.8 (1.5) GPa. And the fibula modulus is 10.2 (1) GPa in the transverse direction (Table 1). The osteons seemed to be stiffer in the femur than in the fibula, possibly because the fibula is not a load-bearing bone. For adult specimens, the mean moduli are: 18.1 (2.6) GPa for osteons, 21.3 (2.3) GPa for interstitial lamellae and 13.8 (1.7) GPa in the transverse direction (Table 1). The elastic moduli for the adults' femurs and for both child bone types (femurs and fibulae) are classified in each of the following directions: longitudinal (osteon and interstitial lamella) and transverse (Table 1). A significant difference between the elastic moduli of adult and child femur specimens in different directions is shown in Table 1. For both adults and children, interstitial bone has a significantly higher modulus than osteonal bone, and the longitudinal modulus of both osteonal and interstitial bone is higher than the transverse modulus (Table 2).

163

164

165

166

167

168

169

170171

172

173

174

175

176

177

178

179

180

181

182

183

184

185

186

187

190

191

192

193

194

195

196

197

198

199

200

201

202

203

204

205

206

207

208

209

210

211

212

213

Discussion

We have assessed the tissue level mechanical properties of non-pathologic cortical bone in children. Bone is known to be a multiscale tissue, with each scale playing a role in bone quality and bone disorders (34). The Haversian structure of long human bones contributes to the anisotropy of mesoscale elastic properties of the cortical part of the bone. However, this elastic anisotropy is also a microscale characteristic of bone tissues. This paper focuses on the microscale level by measuring the mechanical properties of NPCCB specimens in two perpendicular directions. In the literature, indentation protocols vary and entail different parameter values. In most studies, the bone specimens are embedded in epoxy resin, nevertheless it has been proven that the resin, constricts the movement of the collagen fibrils and increases connectivity within the bone material (27). Therefore it changes the bone mechanical properties providing greater bone elastic moduli values. Bone specimens are best prepared without using chemicals for cleaning and without dehydration, thereby preserving the elastic properties of the microstructure features (9). In the present study, the specimens were not embedded in resin. For adult bone, the elastic moduli for osteons 18.1 (2.6) GPa and for interstitial lamellae 21.3 (2.3) GPa in longitudinal direction were lower than those obtained by Rho et al. (2002) (17), 21.8 (2.1) GPa for osteon and 23.8 (1.8) GPa for interstitial lamellae. This difference could be due to the fact that the bone specimens in Rho's study were embedded in epoxy resin (15), whereas the bone specimens in the present work were not embedded and were kept hydrated. In addition to that, the elastic modulus, E*, depends also on the maximum load, the loading/unloading rate and the contact depth, h. For example, Rho et al. (1997) (16) used a load of 13.5 mN with a contact depth of 1000 nm, whereas Bala et al. (2011) (22) chose a maximum load of 500 mN with a contact depth of 5000 nm; both were addressing embedded bone specimens. In this study, the maximum load of 40 mN induced contact depths of roughly 2000 nm, within the range of

214 these literature values. The load chosen in the present work was higher than many other loads in 215 different protocols in the literature (20, 22, 23), since we were seeking to measure a mean value for 216 the elastic moduli in the same way as Bala et al. (2011) (22), avoiding lamellar heterogeneity. To the best of our knowledge it is the first time the elastic moduli of NPCCB are assessed by 217 218 microindentation. Consequently, adults specimens were needed to ensure the reliability of the 219 measurements. The values measured on the adult specimens were close to those reported in Zysset 220 et al. (1999) (18): 19.1 (5.4) GPa for osteons and 21.2 (5.3) GPa for interstitial lamellae on human 221 femur specimens which were not embedded in epoxy resin, were hydrated and have no pathological 222 diseases. Similarly, in accordance with Reisinger et al. (2011) (9) who tested also non-resin, 223 hydrated and non-pathological adult femur specimens, the longitudinal elastic modulus is greater 224 than the elastic modulus measured in transverse direction. Moreover, studies using microindentation as Rho et al. (1997) (16) were done on adult tibiae 225 226 yielding lower moduli for osteons 22.5 (1.3) GPa than for interstitial lamellae 25.8 (0.7) GPa. These 227 tibiae specimens were embedded in epoxy resin and cannot be directly compared to the values obtained in the present work due to the presence of resin and the different bone type. However, the 228 229 ratio between the moduli of the osteonal and the interstitial lamellae of the study can be discussed 230 as reference to the Rho's study since the resin is supposed to act in a similar way on both types of tissue. In both studies, the elastic modulus of the interstitial lamella is greater than the elastic 231 modulus of the osteon. 232 233 Adult femur specimens were used in this study to compare their longitudinal and transverse 234 elastic moduli child femur specimens. The results show a significant difference (Table 1). This different mechanical behavior could be linked to structure changes. Structural parameters varying 235 236 with age include the number of osteons and osteon fragments (35), the percentage of unremodeled 237 bone, and the number of non-Haversian canals or primary osteons (36). Non-Haversian canal

osteons, primary vascular channels filled with concentric lamellae, are known to be present in child

bone and almost disappear in adult bone, unlike the number of osteons, which increases with age

238

240 (37). All the specimens (adult and child) had a greater elastic modulus in the interstitial lamellae 241 than in the osteon, and in the longitudinal than in the transverse direction. 242 Spearman test was used to investigate the correlation between age and elastic moduli for children fibula. Only the elastic modulus of osteon was significantly correlated to age (r=0.4736 for a-243 244 risk=5%). This could be associated to the mineralization of growing bone (38). Significant correlation with age could be found for elastic moduli of interstitial lamellae and transverse but 245 with less confidence 10% and 15% respectively. One of the reasons could be that the interstitial 246 lamellae cannot be distinguished from woven/primary bone which is still present in growing 247 248 cortical bone and could affected the elastic moduli. As the osteons are easily identified in planes 249 perpendicular to the bone axis, the measurement of the elastic modulus is more reliable. Moreover, 250 it is the first microindentation study on NPCCB in literature. This significant correlation is interesting and can be related it to the composition and structure of the growing bone in future 251 252 works. 253 As for animal, the cortical bone becomes stiffer with age (39). The elastic modulus of rabbit cortical bone increases significantly during growth and maturation (40). For porcine femurs, the 254 255 elastic modulus of osteons in young (6 months) and old (42 months) bones (17.5 GPa versus 18 GPa) 256 is lower comparing to the interstitial bone (19 GPa versus 20 GPa). Moreover, the longitudinal 257 elastic modulus of these porcine specimens (18.25 GPa versus 19 GPa) was always higher than in the transverse direction (9 GPa versus 14 GPa). For Casanova et al. (2017) (41), the elastic modulus 258 259 for femoral mice cortical bone in the longitudinal direction is 16 GPa and is higher than that of 12.5 260 GPa in the transverse direction. These observations agree well with the results and other studies 261 addressing bone anisotropy using microindentation (9, 19, 42). 262 Nevertheless, we were unable to further investigate the degree of anisotropy due to the low 263 number of specimens and, above all, because osteon and interstitial lamellae cannot be 264 distinguished in the transverse direction in the indentation protocol. Table 2 therefore compares longitudinal osteon, longitudinal interstitial lamellae and transverse, as proposed by Rho et al. 265

(1999) (32). Another limitation of this work is its use of the Oliver-Pharr method assuming that bone is locally isotropic. A useful direction for further work would be to integrate the anisotropic model (22).

The assessment of the elasticity modulus at the microscopic scale is part of a larger study on multimodal and multi-scale characterization of the NPCCB (33) aimed at obtaining maximum exploitable information from these valuable and rare specimens. Developing a database of multi-scale mechanical properties of children bones will allow making dedicated models to better understand certain pathological mechanisms characteristic of the growing bone (green wood fractures, osteopenia), to improve diagnostic procedures and thus adapt and develop the therapeutic choices: prostheses, orthopedic surgery, and rehabilitation.

An important future goal is to link these microscale parameters to the mesoscale mechanical behavior of bone, using homogenization techniques. Coupled with increasingly effective imaging techniques, this could yield relevant analytical and/or numerical models (43) for the estimation of child bone quality. In addition, both assessing the mechanical parameters and analyzing the degree of anisotropy of cortical bone will be vital to the clinical assessment of bone quality. In conclusion, the contribution of this study lies in determining the elastic moduli for NPCCB specimens at microscale level, providing the first measurements of an indentation modulus in longitudinal and transverse directions.

Acknowledgments

- We are grateful to the Timone Hospital surgery team headed by Professor Franck LAUNAY and to the donors or their legal representatives who gave informed written consent to providing their tissues for investigation, following the acceptance of our experimental protocol by CNIL and ethical approval from the anatomy laboratory. Vincent Long, Magali Gaiani and Angela D'Arienzo provided valuable help in
- setting up experiments. We thank Marjorie Sweetko for English language revision.

Declaration of interest

The authors report no conflicts of interest. The authors alone are responsible for the content and writing of the article.

294 Funding

This work was supported by Carnot Star; and HERMES.

References

- 1. Cowin S. Bone Mechanics HANDBOOK 2nd ed CRC 2001.
- 2. Mitton D, Roux C, Laugier P. Bone Overview in: Laugier, P. Haïat G. (Eds.) Bone Quantitative Ultrasound Springer Netherlands 2011; 1–28.
- 3. Follet H, Boivin G, Rumelhart C, Meunier PJ. The degree of mineralization is a determinant of bone strength: a study on human calcanei. Bone 2004; 34:783–789.
- 4. Currey JD. Role of collagen and other organics in the mechanical properties of bone. Osteoporos 2003; Int 14: 29–36.
- 5. Seeman E. Age- and menopause-related bone loss compromise cortical and trabecular microstructure. J of Gerontology Series A 2013; 68:1218-1225.
- 6. Sobol J, Ptaszynska-Sarosiek I, Charuta A, Oklota-Horba M, Zaba Cz, Niemcunowicz-Janica A. Estimation of age at death: examination of variation in cortical bone histology within the human clavicle. Folia Morphol 2015; 74: 378-388.
- 7. Pathria, M. N., Chung, C. B., & Resnick, D. L. (2016). Acute and stress-related injuries of bone and cartilage: pertinent anatomy, basic biomechanics, and imaging perspective. *Radiology*, 280(1), 21-38.
- 8. Franzoso G, Zysset PK. Elastic anisotropy of human cortical bone secondary osteons Measured by nanoindentation. Journal of Biomechanical Engineering-Transactions of the ASME 2009;131:021001-1-021001-11.
- 9. Reisinger AG, Pahr DH, Zysset PK. Principal stiffness orientation and degree of anisotropy of human osteons based on nanoindentation in three distinct planes. J Mech Behav Biomed Mater Special Issue Soft Tissues Special Issue Section on Soft Tissue 3d Strain 2011; 4:2113–2127.
- 10. Katz JL. Hard tissue as a composite material-I. Bounds on the elastic behavior. Journal of Biomechanics 1971; 4: 455-473.
- 11. Oyen ML. Nanoindentation hardness of mineralized tissues. Journal of Biomechanics 2006; 39: 2699-2702.
- 12. Willems N, Mulder L, Bank RA, Grunheid T, den Toonder JMJ, Zentner A, Langenbach GEJ. Determination of the relationship between collagen cross-links and the bone-tissue stiffness in the porcine mandibular condyle. Journal of Biomechanics 2011; 44: 1132-1136.
- 13. Parnell W, Grimal Q. The influence of mesoscale porosity on cortical bone anisotropy. Investigations via asymptotic homogenization. J R Soc Interface 2008; 6:97-109.
 - 14. Lewis G, Nyman JS. The use of nanoindentation for characterizing the properties of

Mineralized hard tissues: state-of-the art review. Journal of Biomedical Materials Research-Part B: Applied Biomaterials 2008; 87:286-301.

- 15. Ebenstein DM, Pruitt LA. Nanoindentation of biological materials. Nano Today 2006; 1: 26-33.
 - 16. Rho J-Y, Tsui TY, Pharr GM. Elastic properties of human cortical and trabecular lamellaer bone measured by nanoindentation. Biomaterials 1997; 18:1325–1330.
 - 17. Rho JY, Zioupos P, Currey JD, Pharr GM. Microstructural elasticity and regional heterogeneity in human femoral bone of various ages examined by nano-indentation. J Biomech 2002; 35:189–198.
 - 18. Zysset PK, Guo XE, Hoffler CE, Moore K, Goldstein SA. Elastic modulus and hardness of cortical and trabecular bone lamellae measured by nanoindentation in the human femur. J Biomech 1999; 32:1005-1012.
 - 19. Fan Z, Swadener JG, Rho JY, Roy ME, Pharr GM. Anisotropic properties of human Tibial cortical bone as measured by nanoindentation. J Orthop Res 2002; 20:806–810.
 - 20. Hengsberger S, Kulik A, Zysset P. Nanoindentation discriminates the elastic properties of individual human bone lamellae under dry and physiological conditions. Bone 2002; 30:178–184.
 - 21. Dall'Ara E, Öhman C, Baleani M, Viceconti M. The effect of tissue condition and applied load on Vickers hardness of human trabecular bone. J Biomech 2007; 40:3267–3270.
 - 22. Bala Y, Depalle B, Douillard T, Meille S, Clément P, Follet H, Chevalier J, Boivin G. Respective roles of organic and mineral components of human cortical bone matrix in micromechanical behavior: An instrumented indentation study. J Mech Behav Biomed Mater 4 2011; 1473–1482.
 - 23. Fan Z, Smith PA, Eckstein EC, Harris GF. Mechanical properties of OI type III bone tissue measured by nanoindentation. J Biomed Mater Res A 2006; 79A:71–77.
 - 24. Weber M, Roschger P, Fratzl-Zelman N, Schöberl T, Rauch F, Glorieux FH, Fratzl P, Klaushofer K. Pamidronate does not adversely affect bone intrinsic material properties in child with osteogenesis imperfecta. Bone 2006; 39:616–622.
 - 25. Albert C, Jameson J, Toth JM, Smith P, Harris G. Bone properties by nanoindentation in mild and severe osteogenesis imperfecta. Clin Biomech 2013; 28: 110–116.
 - 26. Imbert L, Aurégan J-C, Pernelle K, Hoc T. Mechanical and mineral properties of osteogenesis imperfecta human bones at the tissue level. J Bone 2014; 65:18-24.
 - 27. Bushby AJ, Ferguson VL, Boyde A. Nanoindentation of bone: comparison of specimens tested in liquid and embedded in polymethylmethacrylate. J Matter Res 2004; 19:249-259.
 - 28. Shepherd T, Zhang J, Ovaert T, Roeder R, Niebur G. Direct comparison of nanoindentation and macroscopic measurements of bone viscoelasticity. J Mech Behav Biomed Mater 2011; 4:2055-2062.
- 29. Crandall Keith A, Olaf RP Bininda-Emonds, Georgina M Mace, Robert K Wayne. Considering Evolutionary Processes in Conservation Biology. Trends in Ecology & Evolution 2000; 15:290–95.
- 30. Feng L, Chittenden M, Schirer J, Dickinson M, Jasiuk I. Mechanical properties of Porcine femoral cortical bone measured by nanoindentation. Journal of Biomechanics 2012; 45:1775-1782.
 - 31. Oliver WC, Pharr GM. Measurement of hardness and elastic modulus by Instrumented indentation: Advances in understanding and refinements to methodology. J Mater Res 2004; 19:3–20.
- 38. Rho J-Y, Roy II ME, Tsui TY, Pharr GM. Elastic properties of microstructural components of human bone tissue as measured by nanoindentation. John Wiley &

388 Sons Inc 1999; 45.

- 33. Lefèvre E, Lasaygues P, Baron C, Payan C, Launay F, Follet H, Pithioux M. Analyzing the anisotropic Hooke's law for children's cortical bone. J Mech Behav Biomed Mater 2015; 49:370-377.
 - 34. Karunaratne A, Xi L, Bentley L, Sykes D, Boyde A, Esapa CT, Terrill NJ, Brown SDM, Cox RD, Thakker RV, Gupta HS. Multiscale alterations in bone matrix quality increased fragility in steroid induced osteoporosis. Bone 2016; 84:15-24.
 - 35. Schnitzler CM, Mesquita JM. Cortical porosity in children is determined by age-dependent osteonal morphology. Bone 2013; 55:476-86.
 - 36. Kerley E. The microscopic determination of age in human bone. J Physical Anthropology 1965; 23:149-163.
 - 37. Ingraham M. Histological age estimation of the midshaft clavicle using a new digital technique. 2004; Denton (Texas): University of North Texas.
 - 38. Gourion-Arsiquaud, S., Burket, J. C., Havill, L. M., DiCarlo, E., Doty, S. B., Mendelsohn, R., & Boskey, A. L. (2009). Spatial variation in osteonal bone properties relative to tissue and animal age. Journal of bone and mineral research, 24(7), 1271-1281.
 - 39. Feng, L., Chittenden, M., Schirer, J., Dickinson, M., & Jasiuk, I. (2012). Mechanical properties of porcine femoral cortical bone measured by nanoindentation. Journal of biomechanics, 45(10), 1775-1782.
 - 40. Isaksson, H., Malkiewicz, M., Nowak, R., Helminen, H. J., & Jurvelin, J. S. (2010). Rabbit cortical bone tissue increases its elastic stiffness but becomes less viscoelastic with age. Bone, 47(6), 1030-1038
 - 41. Casanova, M., Balmelli, A., Carnelli, D., Courty, D., Schneider, P., & Müller, R. (2017). Nanoindentation analysis of the micromechanical anisotropy in mouse cortical bone. Royal Society open science, 4(2), 160971.
 - 42. Carnelli, D., Lucchini, R., Ponzoni, M., Contro, R., & Vena, P. (2011). Nanoindentation testing and finite element simulations of cortical bone allowing for anisotropic elastic and inelastic mechanical response. Journal of biomechanics, 44(10), 1852-1858.
 - 43. Skytte TL, Mikkelsen LP, Sonne-Holm S, Wong C. Using a finite element pediatric hip model in clinical evaluation- a feasibility study. J Bioengineer & Biomedical Sci 2017; 7:241.

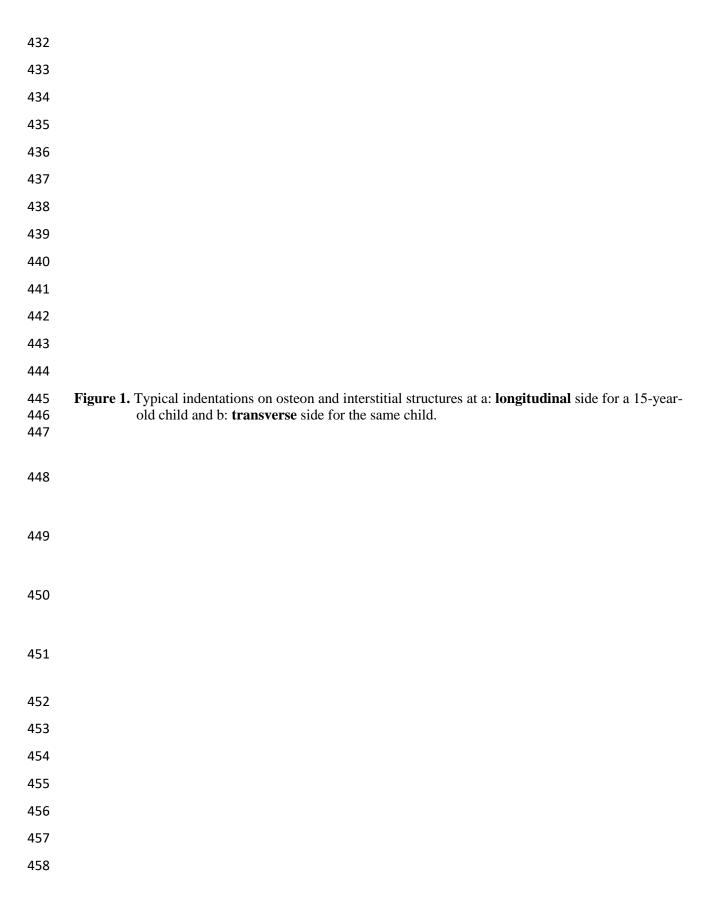


Table 1. Elastic moduli of all adult and child specimens in **longitudinal** and **transverse** directions. P-values for group comparison were obtained using Mann-Whitney test. Bold denotes p-values < 0.05.

| | Adult (femur) (82±8.9) E* Mean (SD*) | Child (femur) (13.3±2.1) E* Mean (SD*) | p-value Adult (femur) and Child (femur) | Child (fibula) (10.2±3.9) E* Mean (SD*) |
|---------------------------|---|---|---|--|
| Longitudinal OSTEON | 18.1 (2.6) | 14.1 (0.8) | 0.024 | 13.5 (1.6) |
| Longitudinal INTERSTITIAL | 21.3 (2.3) | 15.5 (1.5) | 0.142 | 15.8 (1.5) |
| Transverse | 13.8 (1.7) | 11.8 (0.7) | 0.041 | 10.2 (1) |

^{*=}standard deviation.

Table 2. Differences in the elastic moduli between different locations (osteon and interstitial lamellae) and directions (**longitudinal** and **transverse**) of adult and child (fibula) groups using Wilcoxon test.

| | addit dila cilità (110c | Adult | Child |
|------------------|---|--------------|----------------|
| | | (femur) | (fibula) |
| | | (82 ± 8.9) | (10.2 ± 3.9) |
| | | p-value | p-value |
| E* (GPa) | Longitudinal OSTEON versus Longitudinal INTERSTITIAL | 0.011 | 0.0004 |
| <i>E</i> * (GPa) | Longitudinal OSTEON versus Transverse | 0.025 | 0.0004 |
| <i>E</i> * (GPa) | Longitudinal INTERSTITIAL versus Transverse | 0.011 | 0.0004 |